A Peptidomimetic Antagonist of the $\alpha_V\beta_3$ Integrin Inhibits Bone Resorption In Vitro and Prevents Osteoporosis In Vivo

V. Wayne Engleman,* G. Allen Nickols,* F. Patrick Ross,‡ Michael A. Horton,§ David W. Griggs,* Steven L. Settle,* Peter G. Ruminski,* and Steven L. Teitelbaum‡

**Searle Corporation, St. Louis, Missouri 63167; ‡Department of Pathology, Washington University School of Medicine, St. Louis, Missouri 63110; and §Department of Medicine, University College Hospital Medical School, London W1N 8AA, United Kingdom*

Abstract

Osteoclastic bone degradation requires intimacy between the matrix and the resorptive cell. While the precise role the integrin $\alpha_v\beta_3$ plays in the process is not yet understood, occupancy of the heterodimer by soluble ligand or by blocking antibody effectively inhibits bone resorption in vitro and in vivo, suggesting that $\alpha_v\beta_3$ blockade may prevent postmenopausal osteoporosis. Thus, we identified a synthetic chemical peptide mimetic, β-[2-[[5-[(aminoiminomethyl)amino]-1-oxopentyl]amino]-1-oxoethyl]amino-3-pyridinepropanoic acid, bistrifluoroacetate (SC56631) based upon the $\alpha_v\beta_3$ ligand, Arg-Gly-Asp (RGD), which recognizes the isolated integrin, and its relative, $\alpha_v\beta_5$, as effectively as does the natural peptide. The mimetic dampens osteoclastic bone resorption in vitro and in vivo. Most importantly, intravenous administration of the mimetic prevents the 55% loss of trabecular bone sustained by rats within 6 wk of oophorectomy. Histological examination of bones taken from SC56631-treated, oophorectomized animals also demonstrates the compound's bone sparing properties and its capacity to decrease osteoclast number. Thus, an RGD mimetic prevents the rapid bone loss that accompanies estrogen withdrawal. (*J. Clin. Invest.* 1997. 99:2284–2292.) Key words: integrin • osteoclasts • osteoporosis • peptidomimetic

Introduction

Osteoporosis, a disorder of progressive skeletal loss, is characterized by enhanced bone resorption relative to formation. Hence, one may prevent this disease, theoretically, by attenuating the rate by which osteoclasts resorb bone. In fact, this appears to be the case regarding the bone sparing effects of estrogen, presently the most effective antiosteoporotic agent (1).

Reflecting the development of experimental models whereby enriched populations of osteoclasts may be isolated from bone (2) or generated in culture from their hematopoietic progenitors (3, 4), the past decade has witnessed major insights into the ontogeny of the osteoclast and the mechanisms by which it resorbs bone. Specifically, osteoclasts are derived from monocytic precursors that are members of the monocyte/macrophage family (5). Upon contact with bone or other mineralized tissues, the cells multinucleate by fusion, and develop a polarized phenotype unique to the osteoclast's resorptive function (6). Such polarization entails insertion of cytoplasmic vesicles containing an electrogenic H+ATPase (proton pump) similar to that expressed by the intercalated cell of the renal tubule, into the bone-apposed plasma membrane (7). Thus, the resorptive process is initiated by profound acidification of an isolated, extracellular microenvironment at the osteoclast–bone interface. Acidification of this milieu presumably prompts bone mineral mobilization (2) and establishes the pH optimum of osteoclast-residing lysosomal enzymes, such as cathepsin B, which are capable of degrading bone collagen (2, 8). The fact that osteoclastic bone resorption involves a microenvironment with a pH that differs substantially from the general extracellular space (9) indicates that physical intimacy must exist between the osteoclast and the juxtaposed bone matrix, a process probably substantially mediated by integrins.

Integrins are heterodimeric matrix receptors that anchor cells to substrates and transmit externally derived signals across the plasma membrane (10). In a series of experiments involving antibody blockade, we have shown that the integrin $\alpha_v\beta_3$ is essential to the resorptive process, in vivo (11) and in vitro (12,13). This heterodimer recognizes the amino acid motif Arg-Gly-Asp (RGD)[1] contained in bone matrix proteins such as osteopontin and bone sialoprotein (12,13). $\alpha_v\beta_3$ is expressed progressively by osteoclast precursors as they differentiate (14) and its expression is modulated by resorptive steroids and cytokines such as 1,25-dihydroxyvitamin D_3 (15, 16) and granulocyte-macrophage colony stimulating factor, respectively (14).

The fact that peptides containing the RGD motif arrest osteoclastic bone resorption in vitro (12) suggests such agents may also blunt bone resorption in vivo. In fact, shortterm administration of the snake venom protein, echistatin, to mice, blunts the calcemic effect of parathyroid hormone–related peptide (PTHrP) (17, 18). While α_v-associated integrin occupancy has not been shown to be bone sparing in vivo, these findings raise the possibility that small molecular weight, nonbiodegradable RGD mimetics that bind α_v-associated integrins may compete with bone-residing ligands. In so doing, such organic molecules may attenuate osteoclastic bone resorption, thus providing a novel strategy to prevent osteoporosis. We

Address correspondence to Steven L. Teitelbaum, M.D., Department of Pathology, Washington University School of Medicine, Barnes-Jewish Hospital, 216 South Kingshighway, St. Louis, MO 63110. Phone: 314-454-8463; FAX: 314-454-5505; E-mail: teitelbs@medicine.wustl.edu

Received for publication 19 August 1996 and accepted in revised form 6 February 1997.

J. Clin. Invest.

0021-9738/97/05/2284/09 $2.00
Volume 99, Number 9, May 1997, 2284–2292

1. *Abbreviations used in this paper:* G-Pen, Gly-Pen-Gly-Arg-Gly-Asp-Ser-Pro-Cys-Ala (cyclic); OVX, ovariectomy; PTHrP, parathyroid hormone–related peptide; RGD, Arg-Gly-Asp; TPTX, thyroparathyroidectomy; SC56631, β-[2-[[5-[(aminoiminomethyl)amino]-1-oxopentyl]amino]-1-oxoethyl]amino-3-pyridinepropanoic acid, bistrifluoroacetate.

have identified such a mimetic that inhibits bone resorption in vivo and in vitro. Most importantly, when administered to the oophorectomized rat, an animal which, like the postmenopausal patient, is prone to rapid bone loss, this compound completely ablates the osteoporotic effect of estrogen withdrawal. Thus, RGD mimetics, via competition with osteoclast-bearing, α_v-containing integrins present themselves as a new family of antiosteoporotic agents.

Methods

Reagents. Human plasma was obtained from the American Red Cross (St. Louis, MO). Frozen human placenta was obtained from the Department of Pathology, Jewish Hospital (St. Louis, MO). Salmon calcitonin was purchased from Bachem Bioscience, Inc. (King of Prussia, PA) and Gly-Pen-Gly-Arg-Gly-Asp-Ser-Pro-Cys-Ala (cyclic) (G-Pen) from GIBCO BRL (Gaithersburg, MD). The anti-$\alpha_v\beta_3$ blocking murine mAb LM609 was obtained from Telios Pharmaceuticals (La Jolla, CA) and rabbit anti–human β_3 integrin IgG was raised within our group. NHS-biotin was from Pierce Chemical Co. (Rockford, IL). Tris buffer, OPD substrate tablets, and RIA grade BSA were obtained from Sigma Chemical Co. (St. Louis, MO). Peroxidase-labeled and affinity purified antibiotin antibody was obtained from Calbiochem Corp. (La Jolla, CA). PTHrP (1–34), GRGDSP, and GRGDSPK peptides were purchased from Bachem California (Torrance, CA). Linbro microtiter plates were obtained from Flow Laboratories (McLean, VA). The RGD peptidomimetic SC56631 was prepared by medicinal chemists at Searle Corp. (St. Louis, MO). The pyridinoline cross-links assay kit was from Metra Biosystems, Inc. (Mountain View, CA). Ultrafree-MC 10-kD cutoff membranes were purchased from Millipore, Corp. (Bedford, MA).

Purification and biotinylation of human plasma vitronectin. Human vitronectin was purified from fresh frozen plasma (19) and biotinylated by coupling NHS-biotin, from Pierce Chemical Co., to purified vitronectin as previously described (20). Briefly, 1.3 mg of human vitronectin was dissolved in 1.0 ml 0.1 M sodium bicarbonate, 0.1 M NaCl, pH 8.0. NHS–LC-Biotin (300 μg) was added directly to the solution and mixed gently for 1 h at room temperature, followed by overnight incubation at 4°C. The reaction mixture was concentrated in a Centricon 30, diluted with 1 ml PBS, reconcentrated, and finally diluted to 1 ml in PBS containing 0.02% NaN_3. Aliquots were removed for amino acid composition analysis to accurately define the concentration for use in competition experiments. Purification was confirmed by SDS-gel electrophoresis and the ability to bind $\alpha_v\beta_3$ and $\alpha_{IIb}\beta_3$.

Purification of $\alpha_v\beta_3$. Using screened human placental tissue as a source of $\alpha_v\beta_3$, the integrin was purified essentially as described (21). The final eluate from the GRGDSP column was placed in a 14-kD exclusion dialysis bag and concentrated to between 0.5 and 1.0 mg/ml protein versus Aquacide II (Calbiochem Corp.). The concentrate was dialyzed overnight against TBS containing 1 mM $CaCl_2$, 1 mM $MgCl_2$, 1 mM $MnCl_2$, 0.02% sodium azide, and 50 mM octylglucoside, at 4°C. The dialyzed receptor was stable at 4°C for 3 mo or was reconstituted to 10% glycerol and aliquoted for long-term storage at −80°C. Identity of the receptor subunits was confirmed by NH_2-terminal sequence analysis and immunoblot.

Purification of $\alpha_{IIb}\beta_3$. Human fibrinogen receptor ($\alpha_{IIb}\beta_3$) was purified from outdated platelets as previously described (21). After batchwise absorption of a platelet extract with GRGDSPK resin, the resin was washed and eluted with 1 mg/ml GRGDSP peptide. The peptide-eluted receptor was dialyzed to remove peptide and concentrated versus Aquacide II. 20 U of outdated human platelets yields ~700 μg of receptor.

Solid phase receptor assays. As previously reported (22), purified human vitronectin receptor ($\alpha_v\beta_3$) or human fibrinogen ($\alpha_{IIb}\beta_3$) receptors were diluted from stock solutions to 1.0 μg/ml in Tris-buffered saline (TBS) containing 1.0 mM Ca^{2+}, Mg^{2+}, and Mn^{2+}, pH 7.4 (TBS^{3+}). Diluted receptor was immediately transferred to Linbro microtiter plates at 100 μl/well (100 ng receptor per well). The plates were sealed and incubated overnight at 4°C to allow the receptor to bind to the wells. All remaining steps were done at room temperature. The assay plates were emptied and 200 μl of 1% RIA grade BSA in TBS^{3+} (TBS^{3+}/BSA) was added to block exposed plastic surfaces. After a 2-h incubation, the assay plates were washed with TBS^{3+} using a 96-well plate washer. Logarithmic serial dilutions of the test compound and controls were made starting at a stock concentration of 2 mM and using 2 nM biotinylated vitronectin in TBS^{3+}/BSA as the diluent. Premixing of labeled ligand with test (or control) ligand, and subsequent transfer of 50-μl aliquots to the assay plate was undertaken with a CETUS Propette robot; the final concentration of the labeled ligand was 1 nM and the highest concentration of test compound was 10^{-4} M. Competition occurred for 2 h after which all wells were washed with a plate washer. Affinity-purified horseradish peroxidase–labeled goat antibiotin antibody was diluted 1:3,000 in TBS^{3+}/BSA and 125 μl was added to each well. After 30 min, the plates were washed and incubated with OPD/H_2O_2 substrate in 100 mM/liter citrate buffer, pH 5.0. The plate was read, using proprietary software with a microtiter plate reader at a wavelength of 450–630 nm, and when the maximum-binding control wells reached an absorbance of about 1.0, the final $A_{450-630}$ were recorded for analysis. The data were analyzed using a macro written with the EXCEL™ spreadsheet program. The mean, SD, and percentage of CV were determined for duplicate concentrations. The mean A_{450} values were normalized to the mean of four maximum-binding controls (no competitor added). The normalized values were subjected to a four parameter curve fit algorithm (23), plotted on a semi-log scale, and the computed IC_{50} and corresponding r^2 were reported. GRGDSP, a peptide fragment of fibronectin, was included on each plate as a positive control.

Integrin selective cell adhesion assays. Adapting a previously described assay (24), $\alpha_v\beta_3$-dependent adhesion of A3827 melanoma cells to human fibrinogen (10 μg/ml) was measured in 96-well plates in the presence of 200 μM Mn^{2+}. The assay buffer was HBSS containing 0.1% BSA. Cells were preincubated with test compounds or an affinity-purified rabbit anti–human β_3 IgG for 30 min at 37°C before adhesion to fibrinogen. Adhesion proceeded for a period of 30 min at 37°C and, after washing, attached cells were quantitated colorimetrically (450 nm) using *p*-nitrophenyl phosphate as the substrate. Assays were performed in triplicate and each assay was repeated at least three times. Data are reported as a mean IC_{50} value of each triplicate experiment.

The effect of SC56631 on $\alpha_5\beta_1$-mediated adhesion was assessed by inhibition of the previously characterized interaction of human K562 erythroleukemia cells with purified fibronectin (25, 26). The assay was performed essentially as described above, except plates were coated with 5 μg/ml human fibronectin and the number of adherent cells was determined colorimetrically using the CellTiter 96 Cell Proliferation Assay kit (Promega Corp., Madison, WI). Using the same procedure, the effect of the compound on $\alpha_v\beta_1$ function was determined through inhibition of binding of the human embryonic kidney cell line 293, which constitutively expresses this integrin (27), to purified human vitronectin (5.0 μg/ml). An $\alpha_v\beta_5$-specific functional assay similar to that characterized by Hu et al. (28) was developed through stable transfection of the 293 cells with cDNA encoding the human integrin β_5 subunit, and performed as above, in plates coated with 0.3 μg/ml vitronectin. Integrin specificity was confirmed in all cell-based adhesion assays with appropriate control antibodies.

Murine osteoclast bone particle resorption assay. Quantitation of in vitro bone resorption by mouse osteoclasts was performed as described (4). Osteoclasts were generated by coculture, in a total volume of 1 ml, of nonadherent bone marrow macrophages and the murine marrow stromal line ST2 in the presence of 10 nM $1,25(OH)_2D_3$ and 100 nM dexamethasone for 6–8 d. Rat bone particles (100 μg), obtained by powdering dried long bones of rats labeled by injection of ^{3}H-proline (2), were added as a suspension in sterile PBS and me-

dium was removed after 72 h for β scintillation counting. Test compounds or calcitonin, a potent and specific inhibitor of osteoclastic bone resorption (29), was added to selected wells. Resorption was calculated by subtracting the blank count (wells containing labeled bone and no cells) from all samples and expressing the results as a percentage of the zero value (no inhibitor present).

Dentin resorption lacunar assay. Lacunar resorption of sperm whale dentine by neonatal rabbit osteoclasts was assessed using a modified assay as described previously (12). Test reagents were added at the stated final concentrations to the osteoclast cultures after a 40-min settling period to enable adhesion to the dentin slices and were present throughout the 18-h culture period. Kistrin (50 nM) was used as a positive control. The number of resorption lacunae, from six replicate dentin slices for each treatment, was enumerated microscopically after the removal of cells and toluidine blue staining (12); the experiment was repeated twice and data were expressed as a percentage of control (i.e., no reagent addition) values.

Calcemia rat model. All animal procedures were approved by the Institutional Animal Care and Use Committee and conformed to the NIH Guidelines for the Ethical Care and Treatment of Animals. Sprague Dawley rats (250–300 g) were obtained from Charles River Laboratories (Wilmington, MA), allowed to acclimate for at least 3 d, and fasted overnight before experiments. Thyroparathyroidectomy (TPTX) was performed on anesthetized male rats using a ventral, midcervical incision. After ligation of the laryngeal arteries, the thyroid and parathyroid glands were surgically excised and the incision was sutured. The left femoral artery and vein were cannulated to allow for the administration of test compounds (vein) and sampling of blood for circulating calcium concentrations (artery). The animals were placed in Bollman restraining cages and within 18 h after TPTX, serum calcium levels had fallen from 9–10 mg/dl to 5–6 mg/dl. The rats were infused for 5 h with PTHrP (3.5 μg/kg per min) in lactated Ringers to stimulate a calcemic response and to return serum levels to normal. Serum was collected for colorimetric calcium determinations before TPTX, before PTHrP infusion, and at 2, 4, and 5 h. Calcium concentrations of serum samples were determined colorimetrically using a kit from Sigma Chemical Co.

Ovariectomized rat model. 6-mo-old female Sprague Dawley rats were ovariectomized (OVX) on day 0 using a single dorsal incision with bilateral exteriorization of the ovaries ad excision. Sham operated rats had the ovaries exteriorized but not removed. The OVX + Estradiol group were ovariectomized and received silastic implants containing 17β-estradiol (Sigma Chemical Co.), which yielded physiological levels of estrogen (~ 65 pg/ml). The left femoral vein was cannulated, and the cannula was burrowed subcutaneously and exteriorized dorsally at the base of the neck. The animals were active and unrestrained throughout the experiment. OVX experimental groups were continuously infused, intravenously, for 6 wk, with lactated Ringer's solution containing SC56631. The mimetic was delivered at 0.5 (high dose) or 0.1 (low dose) mg/kg per min. Sham operated and OVX control rats were infused at the same rate with solution containing only Ringer's solution. Trabecular bone mineral density was monitored in the rats using peripheral quantitative computerized tomography using a Stratec 960A (Norland, Ft. Atkinson, WI). The rats were anesthetized and trabecular density of the left proximal tibia was performed on day 0 and at 2-wk intervals.

Pyridinoline cross-links assay. 24 h before killing, rats of all experimental groups were transferred to metabolic cages and urine was collected in light protected containers. The samples were analyzed by RIA for pyridinoline cross-link content, using the Pyrilinks™ assay (Metra Biosystems, Inc., Mountain View, CA). The values obtained were normalized to urinary creatinine content.

Quantitation of plasma and urine drug levels. Bioactive concentrations of the drug SC56631 were measured in urine and plasma from drug-treated rats. Samples of urine and serum containing known amounts of SC56631 were used to generate a standard curve. Urine or citrated plasma from drug-treated animals and spiked plasma or urine controls were filtered through 10-kD cut-off membranes (Millipore Corp.) and filtrate was assayed using the $\alpha_v\beta_3$ receptor assay described above.

Human platelet-rich plasma assay. Healthy aspirin-free donors were randomly selected from a pool of volunteers. Harvesting of platelet-rich plasma and subsequent ADP-induced platelet aggregation assays were performed as previously described (30). Standard venipuncture techniques, using a butterfly, allowed withdrawal of 45 ml of whole blood into a 60-ml syringe containing 5 ml of 3.8% trisodium citrate. After thorough mixing in the syringe, the anticoagulated whole blood was transferred to a 50-ml conical polyethylene tube. The blood was centrifuged at room temperature for 12 min at 200 *g* to sediment nonplatelet cells. Platelet-rich plasma was transferred to a polyethylene tube and stored at room temperature until used. Platelet-poor plasma was obtained from a second centrifugation of the remaining blood for 1 min in a tabletop centrifuge. Platelet counts were typically 300,000–500,000 per μl. Platelet-rich plasma (0.45 ml) was aliquoted into siliconized cuvettes and stirred (1,100 rpm) at 37°C for 1 min before adding 50 μl of prediluted test compound. After 1 min of mixing, aggregation was initiated by addition of 50 μl of 200 μM ADP. Aggregation was recorded for 3 min in a dual channel aggregometer (Payton Scientific, Buffalo, NY). The percent inhibition of maximal response (saline control) for a series of test compound dilutions was used to construct a dose–response curve. Active compounds were tested in duplicate in three separate assays and half-maximal inhibition (IC_{50}) was calculated graphically from the dose–response curve.

Rat platelet-rich plasma assay. Rat platelets were prepared in a manner similar to that applied to human platelets. Citrated whole blood, taken from four healthy Sprague Dawley rats, was pooled for each experiment and centrifuged at 350 *g* to sediment nonplatelet cells. Aggregation analysis was identical to that used for human platelets.

Bone histomorphometry. Osteoclast number per millimeter of trabecular surface of proximal tibial metaphyseal bone was histomorphometrically quantitated by the Bioquant system (R & M Biometrics, Inc., Nashville, TN).

Statistics. Significance of differences was calculated by Student's *t* test.

Results

SC56631 recognizes the integrin $\alpha_v\beta_3$. Our first efforts were aimed at identifying nonpeptidic compounds capable of recognizing the integrin, $\alpha_v\beta_3$. To this end we turned to a library of synthetic chemical RGD mimetics, some members of which target the platelet integrin $\alpha_{IIb}\beta_3$, a complex homologous to $\alpha_v\beta_3$. Compounds were screened in the solid phase receptor assay. The most effective, SC56631 (Fig. 1), demonstrates an IC_{50} of 10 nM as regards vitronectin binding to purified $\alpha_v\beta_3$, approximating the potency of GRGDSP and being sixfold less potent than the snake venom protein, echistatin (Fig. 2).

SC56631 blocks substrate attachment of $\alpha_v\beta_3$ expressing cells. Having identified the RGD mimetic that most effectively recognizes $\alpha_v\beta_3$ in solid phase assay, we asked if the compound blocks cell attachment to an $\alpha_v\beta_3$ ligand: fibrinogen. In this circumstance we used A3827 melanoma cells which attach to fibrinogen in an $\alpha_v\beta_3$-dependent manner. As seen in Fig. 3, SC56631 dose-dependently inhibits A3827 cell/fibrinogen binding with an IC_{50} of 120 nM. Complete inhibition of attachment is achieved by a blocking anti-β3 antibody. SC56631

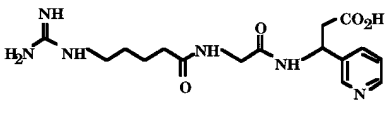

Figure 1. Structure of the synthetic chemical RGD mimetic, SC56631.

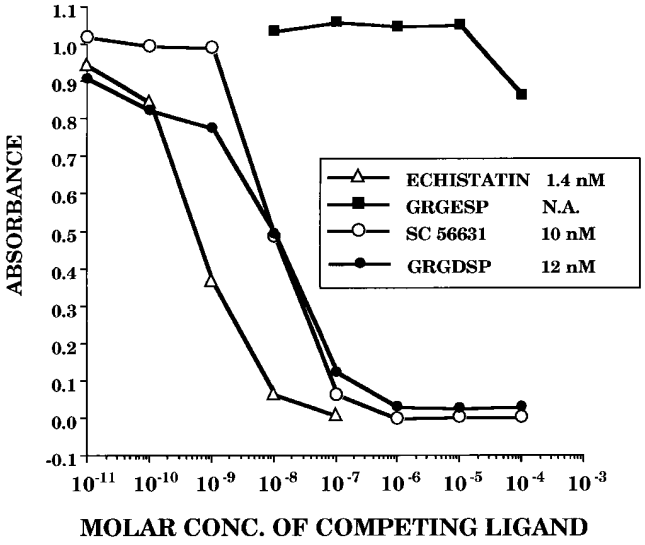

Figure 2. Potency of SC56631 in $\alpha_v\beta_3$ solid phase assay. Plates were coated with purified $\alpha_v\beta_3$ and various test compounds added in the presence of 2.0 nM biotinylated vitronectin. After 2 h, peroxidase-labeled goat antibiotin antibody was added and vitronectin displacement, by test compounds, was determined colorimetrically. Data within the box represent IC_{50} of each potential competing ligand. *N.A.,* not available on basis of data generated. Standard errors of each data point are < 5% of the mean.

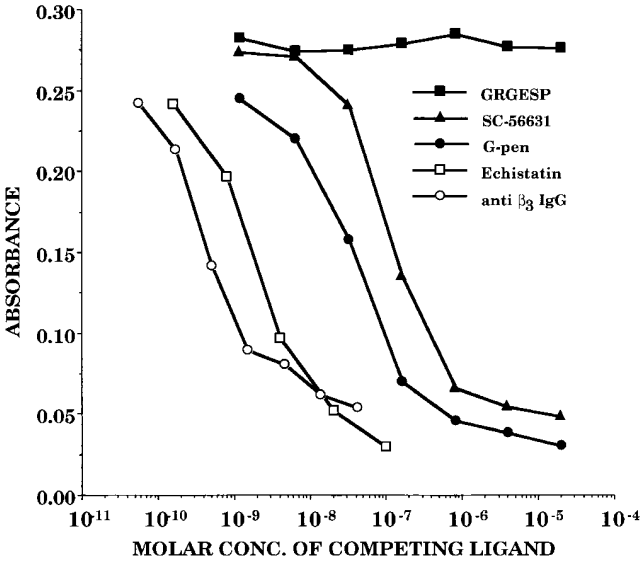

Figure 3. Effect of SC56631 on α_v-dependent adhesion of melanoma cells to fibrinogen. A3827 melanoma cells were preincubated with test compounds for 30 min before addition to fibrinogen-coated wells. 30 min later, the wells were rinsed and cell attachment was colorimetrically determined. Standard errors of each data point are < 5% of the mean.

competitively inhibits biotinylated vitronectin binding to purified human $\alpha_{IIb\beta3}$ with an in vitro IC_{50} of 9 nM but was relatively ineffective in blocking ADP-induced platelet aggregation, in vitro, in human (IC_{50} = 20 μM) or rat (IC_{50} > 300 μM) platelet-rich plasma. The mimetic also dampens attachment of $\alpha_v\beta_1$ expressing 293 cells (IC_{50} = 317 nM) and β_5 transfected 293 cells (IC_{50} = 23 nM). SC56631 has little effect on ligand binding activity of $\alpha_5\beta_1$, inhibiting fibronectin attachment of K562 cells bearing the integrin at an IC_{50} of ~ 70 μM.

SC56631 inhibits bone resorption in vitro. We assessed the capacity of SC56631 to inhibit bone resorption, in vitro, using two assay systems. In the first instance, osteoclasts generated from murine marrow macrophages, cocultured with murine marrow stromal cells, were incubated with devitalized bone prelabeled with ^{3}H-proline. Bone resorption was expressed as a function of cell-mediated isotope release. Substantiating matrix degradation is osteoclast-based, calcitonin inhibits cell-mediated isotope mobilization, dose-dependently, being effective within the physiological range of the hormone (Fig. 4 *A*). We also found that SC56631 progressively blunts osteoclast-mediated bone particle degradation (Fig. 4 *B*) with a potency approximating that of the cyclic RGD peptide, G-Pen (Fig. 4 *C*). Calcitonin (10^{-9} M) and SC56631 (10^{-5} M) fail to impact osteoclast viability as measured by dye exclusion (data not shown).

In the second case, we assessed the capacity of SC56631 to inhibit lacuna formation in dentin by osteoclasts. Similar to the isotope mobilization assay, the peptide mimetic progressively reduces excavation of dentin slices by isolated rabbit osteoclasts (Fig. 5).

SC56631 inhibits bone resorption in vivo. To determine if the RGD mimetic's capacity to inhibit bone resorption in vitro is mirrored in vivo, we turned to the thyroparathyroidectomized rat model described by Harris et al. (31). Total parathyroidectomy was confirmed in each animal by an overnight decline in circulating calcium of at least 3 mg/dl with a mean decrement of 4.8±0.2 mg/dl. As seen in Fig. 6, intravenous infusion of PTHrP (3.5 μg/kg per min), initiated 18 h after TPTX, completely normalizes circulating calcium levels within 5 h. On the other hand, when coinfused, SC56631 dose-dependently dampens the PTHrP-induced calcemic response. In this circumstance, steady state SC56631 plasma levels approximate 1–3 μM, as determined by solid phase assay.

SC56631 prevents oophorectomy-induced osteoporosis. The data presented thus far indicate that the RGD mimetic, SC56631, effectively inhibits osteoclast activity and thus may antagonize development of postmenopausal osteoporosis. Thus, rats were oophorectomized and their bone mineral density was followed with time. Fig. 7 shows these animals experience an ~ 50% loss of trabecular bone mass within 6 wk of surgery, a phenomenon completely inhibited by 17β-estradiol (data not shown). To determine if SC56631 prevents oophorectomy-induced osteoporosis, the animals were constantly infused with the peptidomimetic that is rapidly excreted in urine ($t_{1/2}$ < 20 min). In this circumstance, steady state plasma levels of the active compound, as determined by solid phase assay, approximate 1 and 10 μM for low and high dose administration, respectively. Most importantly, continuous infusion of SC56631 blunts the osteoporotic effect of oophorectomy. Furthermore, urinary excretion of pyridinoline cross-links, a marker of osteoclastic bone resorption, mirrors the magnitude of bone loss in each group (Fig. 8). Reflecting densitometric measurements, histological examination reveals the proximal tibial metaphyses of oophorectomized animals administered 0.5 mg/kg per min SC56631 contain strikingly more bone than those of their untreated counterparts (Fig. 9). The sparing of

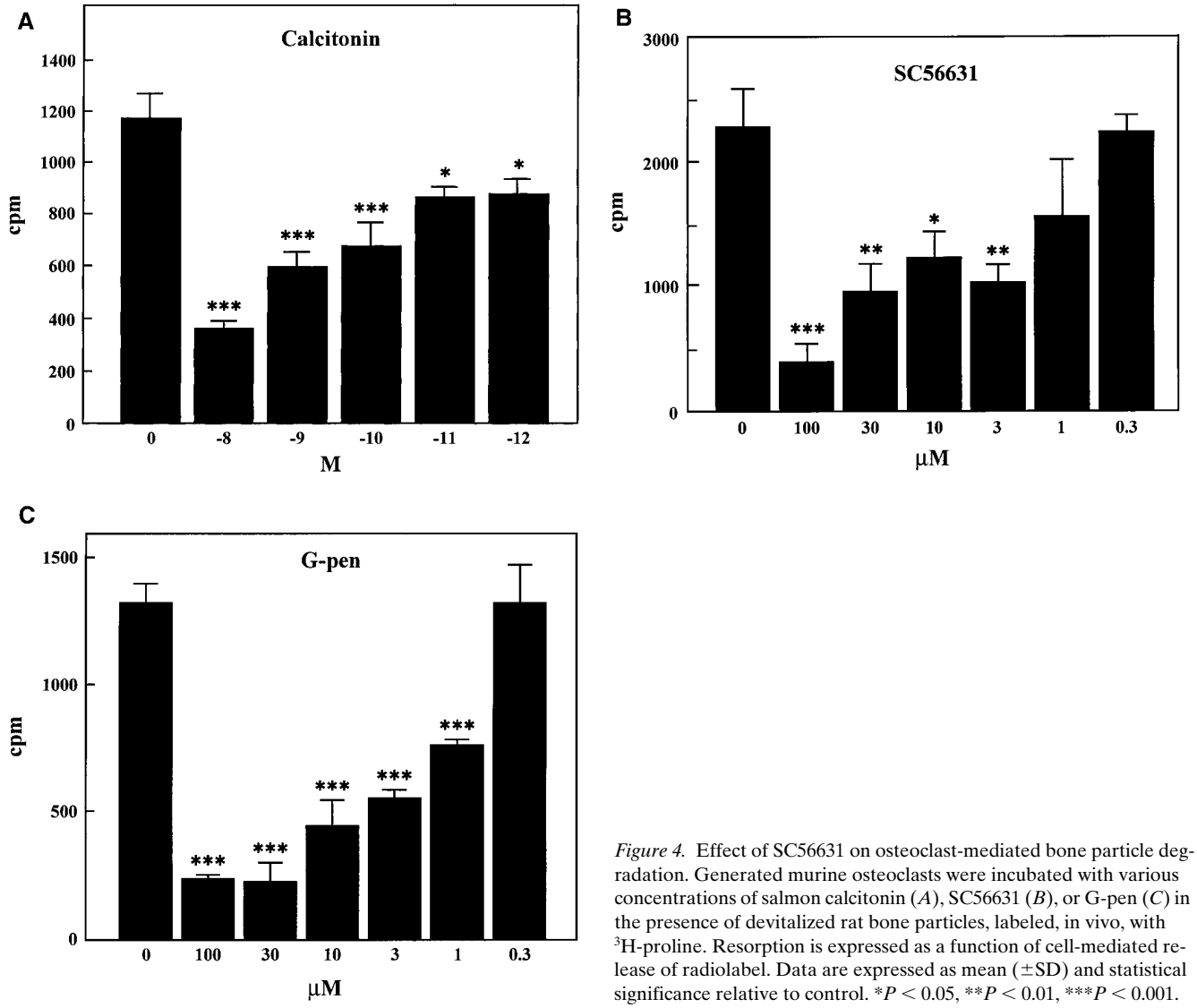

Figure 4. Effect of SC56631 on osteoclast-mediated bone particle degradation. Generated murine osteoclasts were incubated with various concentrations of salmon calcitonin (*A*), SC56631 (*B*), or G-pen (*C*) in the presence of devitalized rat bone particles, labeled, in vivo, with ^{3}H-proline. Resorption is expressed as a function of cell-mediated release of radiolabel. Data are expressed as mean (±SD) and statistical significance relative to control. $*P < 0.05$, $**P < 0.01$, $***P < 0.001$.

oophorectomy-induced bone loss by the mimetic is attended by a reduction in osteoclast number (osteoclast number/mm trabecular surface±SD; ovariectomy = 0.53±0.07; ovariectomy + 0.5 mg/kg per min SC56631 = 0.32±0.04; $P < 0.01$.

Discussion

Bone resorption requires intimacy between matrix and osteoclasts suggesting that the process is integrin mediated. In fact, as evidenced by a host of experimental observations, the $\alpha_v\beta_3$ heterodimer is critical to osteoclastic bone degradation (11–13, 32). However, a great deal remains to be learned regarding the precise role the integrin plays in osteoclast function. Much of this confusion reflects the anatomical distribution of $\alpha_v\beta_3$ on the resorptive polykaryon.

During the process of differentiation and polarization, the osteoclast develops a distinct anatomical structure, the sealing, or "clear," zone, which probably anchors the cell to bone and isolates the resorptive microenvironment from the general extracellular space (33). While its molecular composition is not yet understood (34), the sealing zone, which is actin rich (35), is believed to contain cellular molecules essential to osteoclast-bone recognition. On the other hand, while some investigators report $\alpha_v\beta_3$ presence in this structure (36), others claim the integrin, which is present on the nonbone apposed plasma membrane, is absent in the sealing zone (37, 38).

The latter contention, if true, suggests that $\alpha_v\beta_3$ plays a resorptive role other than osteoclast anchoring. In fact, the osteoclast integrin transmits signals derived from soluble RGD-containing proteins, such as osteopontin (10). In this regard, a reasonable hypothesis holds that $\alpha_v\beta_3$ occupancy by soluble products of matrix resorption terminates skeletal degradation by inducing the osteoclast to withdraw from the bone surface—a finding supported by the prominent basal lateral distribution of $\alpha_v\beta_3$ in resorbing osteoclasts. Whether or not the heterodimer functions as an anchoring and/or signaling molecule in the resorptive process still must be resolved.

Regardless of the means by which $\alpha_v\beta_3$ governs osteoclast activity, its occupancy by peptide ligands attenuates the process (12, 39). Moreover, a 6-h infusion of the $\alpha_v\beta_3$ ligand, echistatin, dampens parathyroid hormone–mediated hypercalcemia in the thyroparathyroidectomized rat (17). Before this

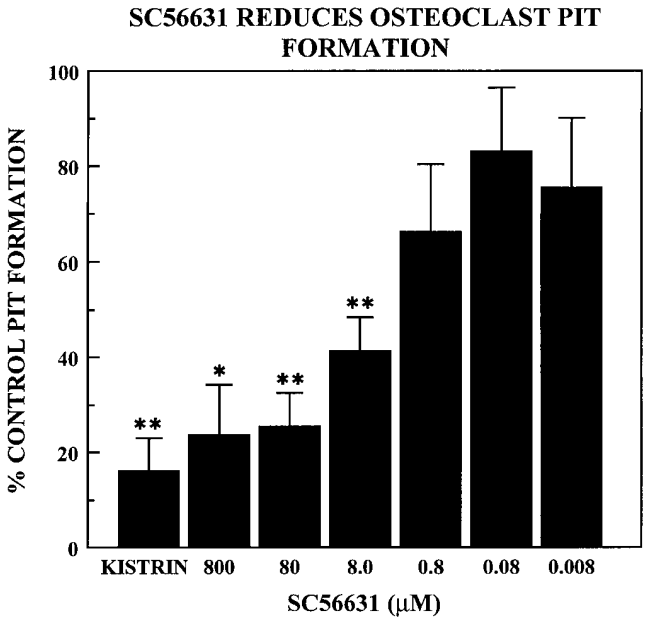

Figure 5. Effect of SC56631 on osteoclast-mediated dentin resorption lacunae formation. Isolated rabbit osteoclasts were incubated for 18 h on sperm whale dentin slices in the presence of various concentrations of SC56631. Addition of kistrin (50 nM) served as positive control. The number of resorption lacunae in each of six slices was determined. Data are expressed as mean percentage (±SD) of negative control, namely the number of resorption pits formed in the absence of added reagent. Statistical significance is expressed relative to negative control. $*P < 0.05$, $**P < 0.01$.

report, α_v integrin antagonists had not been shown to be skeletal sparing.

Patients in the years immediately after menopause experience their most profound loss of bone, reflecting, in this instance, absolute acceleration of osteoclast activity (40). In fact, the most effective antiosteoporotic agent known, estrogen, exerts its bone sparing effect by curbing resorption, an event probably reflecting suppressed recruitment of osteoclast precursors (41).

These observations prompted us to hypothesize that blockade of the osteoclast $\alpha_v\beta_3$ integrin may be bone sparing in states of estrogen depletion. Given the resistance of RGD mimetics to proteolytic degradation, we chose to focus on these compounds rather than more labile peptides.

The similarity in structure (42) and ligand recognition of $\alpha_v\beta_3$ and the platelet integrin, $\alpha_{11b}\beta_3$, which also recognizes the RGD motif, prompted us to screen a library of mimetics devel-

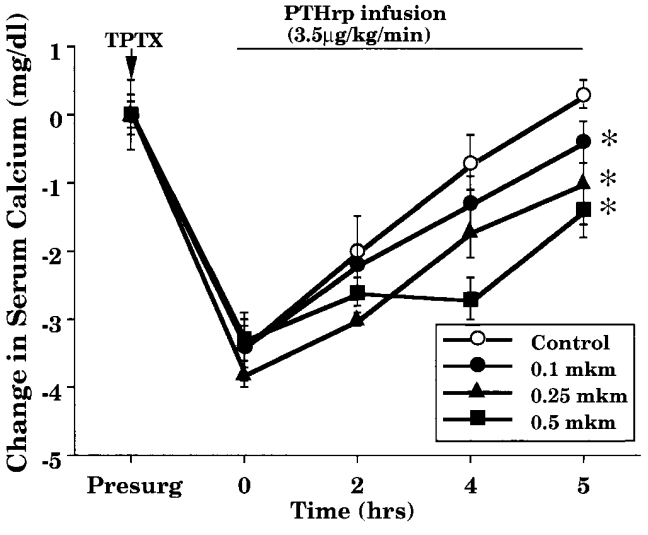

Figure 6. Effect of SC56631 on PTHrP-mediated calcemia. Rats subjected to TPTX 18 h earlier were infused with PTHrP (3.5 μg/kg per min) in the presence of various concentrations of SC56631. Serum calcium levels were determined before TPTX, at the start of infusion, and 2, 4, and 5 h thereafter. $*P < 0.01$ relative to control at 5 h. *mkm*, Mg/kg per min.

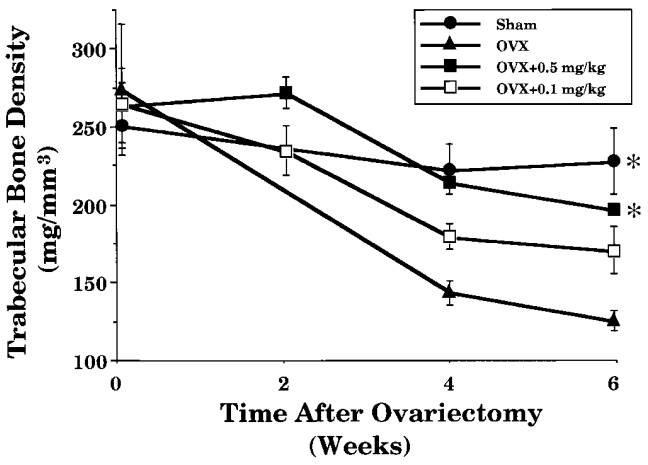

Figure 7. Effect of SC56631 on oophorectomy-induced bone loss. Rats were sham operated or subjected to oophorectomy. Oophorectomized animals were either untreated (*OVX*), supplemented with 17β-estradiol, or infused with either 0.5 or 0.1 mg/kg per min (mkm) SC56631. Trabecular bone density was measured by pQCT at initiation of the study and with time. Data are presented as mean±SD. $*P < 0.001$ relative to OVX at 6 wk.

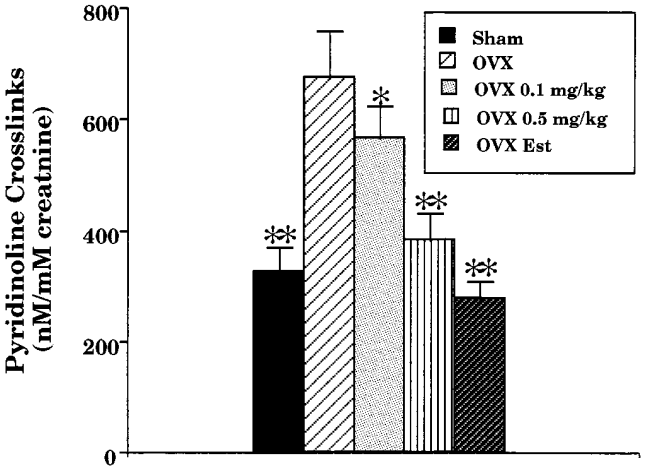

Figure 8. Effect of SC56631 on pyridinoline cross-link excretion. Urine was collected from rats described in Fig. 7 before killing, 6 wk after OVX or sham operation. Pyridinoline cross-link content, normalized to creatinine, was measured by ELISA. Data are presented as mean±SEM. $*P < 0.01$, $**P < 0.001$ relative to OVX.

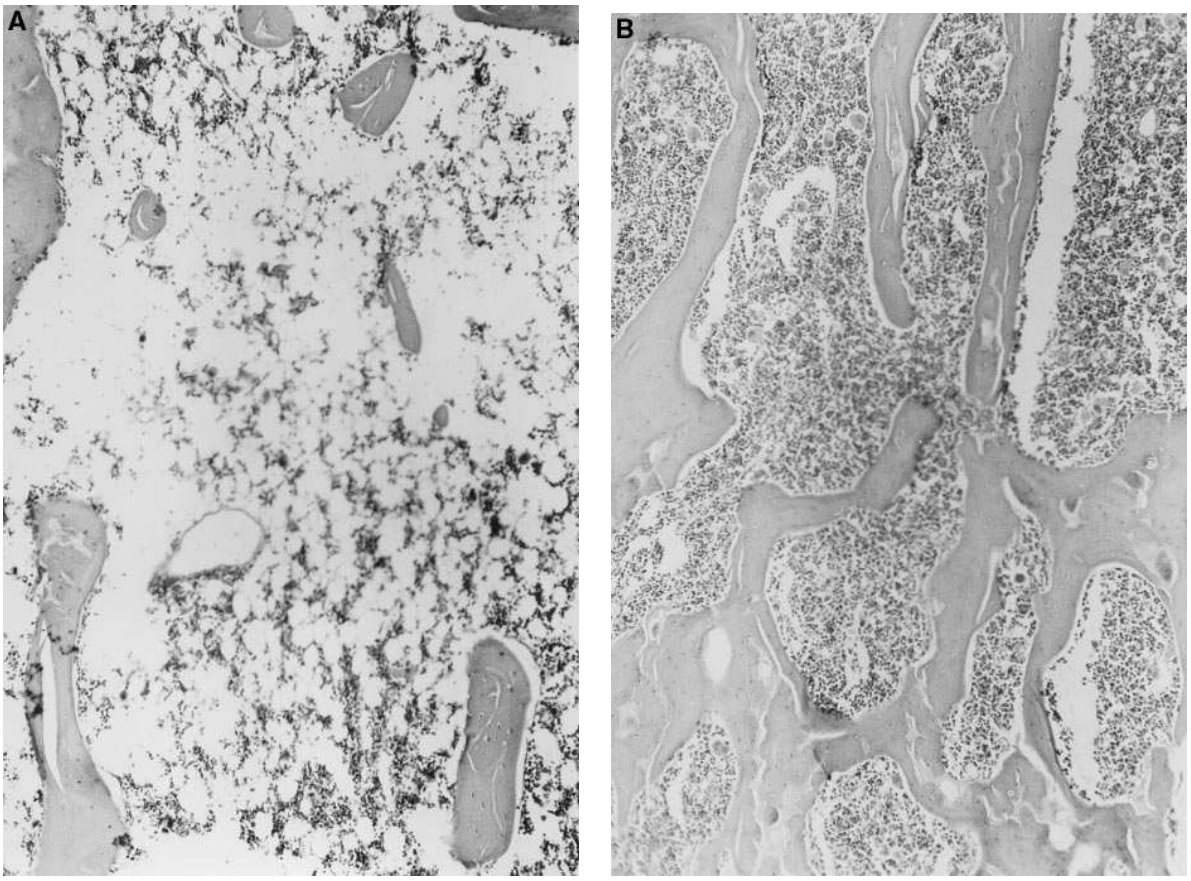

Figure 9. Histological effect of SC56631. Proximal tibiae from control oophorectomized rats (*A*) and those infused with 0.5 mg/kg per min SC56631 (*B*) were decalcified and histological sections were prepared. Untreated oophorectomized rats are osteoporotic as evidenced by the presence of small individual islands of cancellous bone with loss of connectivity between trabeculae. In comparison, bones of SC56631 infused animals exhibit numerous, well-connected trabeculae. Hematoxylin and eosin, ×40.

oped to occupy the latter heterodimer and thus to prevent pathological clotting. Using a rapid solid phase assay consisting of immobilized $\alpha_v\beta_3$ and biotinylated vitronectin, we were able to identify an RGD mimetic which inhibits ligand binding as effectively as the native peptide sequence does. Interestingly, while SC56631 fails to discriminate between the osteoclast and platelet β_3 integrins, we observed no bleeding in rats that were administered the compound for as long as 6 wk. The discrepancy between effective solid phase recognition of $\alpha_{IIb}\beta_3$ by SC56331 and the absence of bleeding, in treated animals, likely relates to our observation that in vitro IC_{50} values, determined with the purified human integrin, are significantly lower than those obtained in vivo or ex vivo (43). Such differences may reflect activation of the purified receptor or the need for $>$ 50% $\alpha_{IIb}\beta_3$ occupancy to suppress fibrinogen-mediated platelet aggregation. Moreover, the fact that at least 15 times more SC56631 is required to achieve half-maximal inhibition of rat, as compared to human platelet aggregation, suggests that rats are relatively coagulation prone.

Having identified a putative $\alpha_v\beta_3$ antagonist by solid phase assay, we asked if its function extends to intact cells. We found that the candidate molecule diminishes binding of $\alpha_v\beta_3$-expressing melanoma cells to one of the integrin's ligands, fibrinogen, at an IC_{50} approximating the mimetic's affinity for the heterodimer. Although somewhat less effectively than for $\alpha_v\beta_3$, the mimetic also competes for $\alpha_v\beta_1$, an osteoclast bearing integrin participating in the resorptive process (44).

Having established the inhibitory properties of SC56631 on osteoclast-matrix adhesion, we turned to the more distal and clinically significant event of resorption. To this end, we exploited two in vitro assays, each focusing on bone matrix degradation. In the first instance, we used the more quantitative approach of cell-mediated mobilization, from bone particles of matrix proteins, a process preceded by demineralization (7). Importantly, physiological concentrations of the antiresorptive hormone, calcitonin, diminish matrix mobilization in this assay.

SC56631 inhibits osteoclast-mediated bone particle degradation with a potency mirroring that of G-Pen, a cyclic RGD peptide which blunts resorption in organ culture (45). In an assay less quantitative but more representative of osteoclast function in vivo, the mimetic also dampens the cell's capacity to form lacunae in dentin. In keeping with the observations of Sato and co-workers who find osteoclast mediated particle degradation and lacuna formation reflective of each other (46), the IC_{50} value of SC56631 is similar in both assays.

Our most compelling evidence supporting the candidacy of RGD mimetics as potential antiosteoporotic agents comes from in vivo experiments. SC56631, a small molecule, is rap-

idly excreted in urine. However, we were, by constant infusion, able to attain effective circulating levels approximating 1.0–10 μM in plasma. Similar to echistatin, SC56631 blunts PTHrP-stimulated calcemia in the thyroparathyroidectomized rat. Most importantly, our experiments are first to establish that an $\alpha_v\beta_3$ antagonist prevents osteoporosis, and does so as effectively as estrogen. These densitometric observations are mirrored by excretion of pyridinoline cross-links, a sensitive marker of bone degradation.

Similar to menopausal women, the oophorectomized rat contains abundant osteoclasts juxtaposed to bone and residing in resorption bays. Our data indicate that SC56631 not only blocks the resorptive activity of mature osteoclasts, but also reduces their number. This dual effect of SC56631 on osteoclast biology may reflect the mimetic's high affinity recognition of both $\alpha_v\beta_3$ and $\alpha_v\beta_5$. We find that osteoclast precursors express $\alpha_v\beta_5$ as their dominant α_v-associated integrin to be replaced, on the mature osteoclast, by $\alpha_v\beta_3$ (14). Furthermore, $\alpha_v\beta_5$ appears to mediate attachment of osteoclast precursors to matrix, an event that is fundamental to their differentiation (14). The capacity of SC56631 to decrease osteoclast number and resorptive activity suggests that the mimetic exerts its bone sparing effects by competing for both α_v-associated integrins.

Acknowledgments

This study was supported in part by NIH grants AR32788, DE05413, and a grant from the Shriners Hospital for Crippled Children, St. Louis Unit (S.L. Teitelbaum), Monsanto/Washington University Biomedical Grant, NIH grants AR42404, AR42356 (F.P. Ross), and the Wellcome Trust (M.A. Horton).

References

1. Wronski, T.J., M. Cintron, A.L. Doherty, and L.M. Dann. 1988. Estrogen treatment prevents osteopenia and depresses bone turnover in ovariectomized rats. *Endocrinology.* 123:681–686.

2. Blair, H.C., A.J. Kahn, E.C. Crouch, J.J. Jeffrey, and S.L. Teitelbaum. 1986. Isolated osteoclasts resorb the organic and inorganic components of bone. *J. Cell Biol.* 102:1164–1172.

3. Alvarez, J.I., S.L. Teitelbaum, H.C. Blair, E.M. Greenfield, N.A. Athanasou, and F.P. Ross. 1991. Generation of avian cells resembling osteoclasts from mononuclear phagocytes. *Endocrinology.* 128:2324–2335.

4. Shioi, A., F.P. Ross, and S.L. Teitelbaum. 1994. Enrichment of generated murine osteoclasts. *Calcif. Tissue Int.* 55:387–394.

5. Udagawa, N., N. Takahashi, T. Akatsu, H. Tanaka, T. Sasaki, T. Nishihara, and T. Koga. 1990. Origin of osteoclasts: mature monocytes and macrophages are capable of differentiating into osteoclasts under a suitable microenvironment prepared by bone marrow-derived stromal cells. *Proc. Natl. Acad. Sci. USA.* 87:7260–7264.

6. Fallon, M.D., S.L. Teitelbaum, and A.J. Kahn. 1983. Multinucleation enhances macrophage-mediated bone resorption. *Lab. Invest.* 49:159–164.

7. Blair, H.C., S.L. Teitelbaum, R. Ghiselli, and S. Gluck. 1989. Osteoclastic bone resorption by a polarized vacuolar proton pump. *Science (Wash. DC.).* 245:855–857.

8. Blair, H.C., S.L. Teitelbaum, L.E. Grosso, D.L. Lacey, H. Tan, D.W. McCort, and J.J. Jeffrey. 1993. Extracellular matrix degradation at acid pH: avian osteoclast acid collagenase isolation and characterization. *Biochem. J.* 290:873–884.

9. Silver, I.A., R.J. Murrills, and D.J. Etherington. 1988. Microelectrode studies on the acid microenvironment beneath adherent macrophages and osteoclasts. *Exp. Cell Res.* 175:266–276.

10. Miyauchi, A., J. Alvarez, E.M. Greenfield, A. Teti, M. Grano, S. Colucci, A. Zambonin-Zallone, F.P. Ross, S.L. Teitelbaum, and D. Cheresh. 1991. Recognition of osteopontin and related peptides by an $\alpha_v\beta_3$ integrin stimulates immediate cell signals in osteoclasts. *J. Biol. Chem.* 266:20369–20374.

11. Crippes, B.A., V.W. Engleman, S.L. Settle, J. Delarco, R.L. Ornberg, M.H. Helfrich, M.A. Horton, and G.A. Nickols. 1996. Antibody to β_3 integrin inhibits osteoclast-mediated bone resorption in the thyroparathyroidectomized rat. *Endocrinology.* 137:918–924.

12. Horton, M.A., M.L. Taylor, T.R. Arnett, and M.H. Helfrich. 1991. Arg-gly-asp (RGD) peptides and the anti-vitronectin receptor antibody 23C6 inhibit dentine resorption and cell spreading by osteoclasts. *Exp. Cell Res.* 195:368–375.

13. Ross, F.P., J.I. Alvarez, J. Chappel, D. Sander, W.T. Butler, M.C. Farach-Carson, K.A. Mintz, P.G. Robey, S.L. Teitelbaum, and D.A. Cheresh. 1993. Interactions between the bone matrix proteins osteopontin and bone sialoprotein and the osteoclast integrin $\alpha_v\beta_3$ potentiate bone resorption. *J. Biol. Chem.* 268:9901–9907.

14. Inoue, M., S.L. Teitelbaum, L. Hurter, K. Hruska, E. Seftor, M. Hendrix, and F.P. Ross. 1995. GM-CSF regulates expression of the functional integrins $\alpha_v\beta_3$ and $\alpha_v\beta_5$ in a reciprocal manner during osteoclastogenesis. *J. Bone Miner. Res.* 10:S163*a.* (Abstr.)

15. Mimura, H., X. Cao, F.P. Ross, M. Chiba, and S.L. Teitelbaum. 1994. $1,25(OH)_2D_3$ vitamin D_3 transcriptionally activates the β_3-integrin subunit gene in avian osteoclast precursors. *Endocrinology.* 134:1061–1066.

16. Cao, X., F.P. Ross, L. Zhang, P.N. MacDonald, J. Chappel, and S.L. Teitelbaum. 1993. Cloning of the promoter for the avian integrin β_3 subunit gene and its regulation by 1,25-dihydroxyvitamin D_3. *J. Biol. Chem.* 268:27371–27380.

17. Fisher, J.E., M.P. Caulfield, M. Sato, H.A. Quartuccio, R.J. Gould, V.M. Garsky, G.A. Rodan, and M. Rosenblatt. 1993. Inhibition of osteoclastic bone resorption in vivo by echistatin, an "arginyl-glycyl-aspartyl" (RGD)-containing protein. *Endocrinology.* 132:1411–1413.

18. Yamamoto, M., R. Balena, A. Markatos, M. Gentile, V.M. Garsky, and G.A. Rodan. 1993. Direct demonstration of inhibitory effect of echistatin on PTH-induced bone resorption in vivo in mice. *J. Bone Miner. Res.* 8:S123*a* (Abstr.)

19. Yatohgo, T., M. Izumi, H. Kashiwagi, and M. Hayashi. 1988. Novel purification of vitronectin from human plasma by heparin affinity chromatography. *Cell Struct. Func.* 13:281–293.

20. Charo, I.F., L. Nannizzi, D.R. Phillips, M.A. Hsu, and R.M. Scarborough. 1991. Inhibition of fibrinogen binding to GP IIb/IIIa by a GP IIIa peptide. *J. Biol. Chem.* 266:1415–1421.

21. Pytela, R., M.D. Pierschbacher, S. Argraves, S. Suzuki, and E. Ruoslahti. 1987. Arginine-glycine-aspartic acid adhesion receptors. *Methods Enzymol.* 144:475–489.

22. Niiya, K., E. Hodson, R. Bader, V. Byers-Ward, J.A. Koziol, E.F. Plow, and Z.M. Ruggeri. 1987. Increased surface expression of the membrane glycoprotein IIb/IIIa complex induced by platelet activation: relationships to the binding of fibrinogen and platelet aggregation. *Blood*. 70:475–483.

23. Rodbard, D., P.J. Munson, and A. de Lean. 1977. Improved curve fitting, parallelism testing, characterization of sensitivity and specificity, validation, and optimization for radioligand assays. *In* Radioimmunoassay and Related Procedures in Medicine. Atomic Energy Agency, Vienna. 469 pp.

24. Lampugnani, M.G., S. Bernasconi, P. Neri, L. Lozzi, I. Gavassi, P.C. Marchisio, and E. Dejana. 1991. Role of manganese in MG-63 osteosarcoma cell attachment to fibrinogen and von Willebrand factor. *Lab. Invest.* 65:96–103.

25. Blystone, S.D., I.L. Graham, F.P. Lindberg, and E.J. Brown. 1994. Integrin alpha v beta 3 differentially regulates adhesive and phagocytic functions of the fibronectin receptor alpha 5 beta 1. *J. Cell Biol.* 127:1129–1137.

26. Mould, A.P., S.K. Akiyama, and M.J. Humphries. 1995. Regulation of distinct $\alpha_5\beta_1$-fibronectin interactions by divalent cations. *J. Biol. Chem.* 270: 26270–26277.

27. Bodary, S.C., and J.W. McLean. 1990. The integrin β_1 subunit associates with the vitronectin receptor α_v subunit to form a novel vitronectin receptor in a human embryonic kidney cell line. *J. Biol. Chem.* 265:5938–5941.

28. Hu, D.D., E.C.K. Lin, N.L. Kovach, J.R. Hoyer, and J.W. Smith. 1995. A biochemical characterization of the binding of osteopontin to integrins $\alpha_v\beta_1$ and $\alpha_v\beta_5$. *J. Biol. Chem.* 270:26232–26238.

29. Fenton, A.J., T.J. Martin, and G.C. Nicholson. 1993. Long-term culture of disaggregated rat osteoclasts: inhibition of bone resorption and reduction of osteoclast-like cell number by calcitonin and PTHrP[107–139]. *J. Cell. Physiol.* 155:1–7.

30. Zucker, M.B. 1989. Platelet aggregation measured by the photometric method. *Methods Enzymol.* 169:117–133.

31. Harris, R.A., D.L. Cares, and L.R. Forte. 1981. Reduction of brain calcium after consumption of diets deficient in calcium or vitamin D. *J. Neurochem.* 36:460–466.

32. Nesbitt, S., A. Nesbit, M. Helfrich, and M. Horton. 1993. Biochemical characterization of human osteoclast integrins. Osteoclasts express $\alpha_v\beta_3$, $\alpha_2\beta_1$, and $\alpha_v\beta_1$ integrins. *J. Cell Biol.* 268:16737–16745.

33. Holtrop, M.E., and L.G. Raisz. 1979. Comparison of the effects of 1,25-dihydroxycholecalciferol, prostaglandin E_2, and osteoclast-activating factor with parathyroid hormone on the ultrastructure of osteoclasts in cultured long bones of fetal rats. *Calcif. Tissue Int.* 29:201–205.

34. Vaananen, H.K., and M. Horton. 1995. The osteoclast clear zone is a specialized cell-extracellular matrix adhesion structure. *J. Cell Sci.* 108:2729–2732.

35. Holtrop, M.E., K.A. Cox, M.B. Clark, M.F. Holick, and C.S. Anast. 1981. 1,25-Dihydroxycholecalciferol stimulates osteoclasts in rat bones in the absence of parathyroid hormone. *Endocrinology.* 108:2293–2301.

36. Reinholt, F.P., K. Hultenby, A. Oldberg, and D. Heinegard. 1990. Osteopontin—a possible anchor of osteoclasts to bone. *Proc. Natl. Acad. Sci.*

USA. 87:4473–4475.

37. Masarachia, P., M. Yamamoto, G.A. Rodan, and L.T. Duong. 1995. Colocalization of the vitronectin receptor $\alpha_v\beta_3$ and echistatin in osteoclasts during bone resorption in vivo. *J. Bone Miner. Res.* 10:S164*a* (Abstr.)

38. Lakkakorpi, P.T., M.A. Horton, M.H. Helfrich, E.-K. Karhukorpi, and H.K. Vaananen. 1991. Vitronectin receptor has a role in bone resorption but does not mediate tight sealing zone attachment of osteoclasts to the bone surface. *J. Cell Biol.* 115:1179–1186.

39. Sato, M., M.K. Sardana, W.A. Grasser, V.M. Garsky, J.M. Murray, and R.J. Gould. 1990. Echistatin is a potent inhibitor of bone resorption in culture. *J. Cell Biol.* 111:1713–1723.

40. Riggs, B.L., and L.J. Melton. 1986. Evidence for two distinct syndromes of involutional osteoporosis. *Am. J. Med.* 75:899–901.

41. Jilka, R.L., G. Hangoc, G. Girasole, G. Passeri, D.C. Williams, J.S. Abrams, B. Boyce, H. Broxmeyer, and S.C. Manolagas. 1992. Increased osteoclast development after estrogen loss: mediation by interleukin-6. *Science (Wash. DC)*. 257:88–91.

42. Fitzgerald, L.A., B. Steiner, S.C. Rall, Jr., S.S. Lo, and D.R. Phillips. 1987. Protein sequence of endothelial glycoprotein IIIa derived from a cDNA clone. Identity with platelet glycoprotein IIIa and similarity to "integrin." *J. Biol. Chem.* 87:3936–3939.

43. Nicholson, N.S., S.G. Panzer-Knodle, L.W. King, B.B. Taite, B.T. Keller, F.S. Tjong, V.W. Engleman, T.D. Giorgio, and L.P. Feigan. 1994. A potent and specific inhibitor of platelet aggregation. *Thromb. Res.* 74:523–535.

44. Helfrich, M.H., S.A. Nesbitt, P.T. Lakkakorpi, M.J. Barnes, S.C. Bodary, G. Shankar, W.T. Mason, D.L. Mendrick, H.K. Vaananen, and M.A. Horton. 1996. β_1 integrins and osteoclast function: involvement in collagen recognition and bone resorption. *Bone (NY)*. 19:317–328.

45. van der Pluijm, G., H. Mouthaan, C. Baas, H. de Groot, S. Papapoulos, and C. Lowik. 1994. Integrins and osteoclastic resorption in three bone organ cultures: differential sensitivity to synthetic Arg-Gly-Asp peptides during osteoclast formation. *J. Bone Miner. Res.* 9:1021–1028.

46. Hiura, K., S.S. Lim, S.P. Little, S. Lin, and M. Sato. 1995. Differentiation dependent expression of tensin and cortactin in chicken osteoclasts. *Cell Motil. Cytoskeleton.* 30:272-284.